International Journal of Earth Sciences (2020) 109:2643–2658
https://doi.org/10.1007/s00531-020-01853-5

ORIGINAL PAPER

Small-scale slope instability on the submarine flanks of insular volcanoes: the case-study of the Sciara del Fuoco slope (Stromboli)

Daniele Casalbore[1] · Flavio Passeri[1] · Paolo Tommasi[1] · Luca Verrucci[2] · Alessandro Bosman[1] · Claudia Romagnoli[3] · Francesco Latino Chiocci[4]

Received: 30 September 2019 / Accepted: 14 March 2020 / Published online: 31 March 2020

Abstract
Small-scale landslides affecting insular and coastal volcanoes are a relevant geohazard for the surrounding infrastructures and communities, because they can directly impact them or generate local but devastating tsunamis, as demonstrated by several historical accounts. Here, a review of such landslides and associated predisposing/triggering mechanisms is presented, with particular reference to the submarine volcanic flanks. We take into account, as a case study, the instability phenomena occurring on the Sciara del Fuoco (SdF, hereafter), a 2-km wide subaerial-submarine collapse scar filled by volcaniclastic products, which form the NW flank of the Stromboli volcano. Because of its steepness (> 30°) and the high amount of loose volcanic material funneled from the summit crater towards the sea, the submarine part of the SdF is prone to instability phenomena recurring at different spatial and temporal scale. Particularly, landsides with a volume of some millions of cubic meters, as the 2002 tsunamigenic landslide, can repeatedly affect the submarine slope. Based on the integration of 11 years (2002–2013) of morpho-bathymetric monitoring of the SdF with geotechnical characterization of volcaniclastic and lava flow materials, stability analyses of the subaerial and submarine slope and previous literature studies, we analyze the role of different triggering mechanisms in controlling the occurrence and size of submarine slope failures at the SdF, such as dykes intrusion as occurred in 2002 or the emplacement of a large delta as occurred in 2007.

Keywords Multibeam bathymetry · Slope stability · Tsunamigenic landslide · Lava delta · Time-lapse surveys · Stromboli · Geotechnical modelling

Introduction

Volcanic eruptions, landslides and associated tsunamis are recognized as one of the main geohazards on insular volcanoes, and a source of risk for surrounding areas. Several natural disasters (with more than 40,000 casualties only in the last few centuries) have been the direct or indirect result of landslides affecting volcanic flanks, as observed at Oshima–Oshima in 1741 and Unzen Volcano in 1792 (Japan) (Satake and Kato 2001; Satake 2007; Brantley and Scott 1993; Sassa et al. 2016), Krakatau in 1883 and Anak Krakatau in 2018 (Indonesia) (Self and Rampino 1981; Walter et al. 2019), Ritter Island in 1888 and Sissano in 2002 (Papua New Guinea) (Tappin et al. 2001; Karstens et al. 2019), St. Augustine in 1883 (Alaska) (Beget and Kienle 1992) to name a few.

Because of their huge volume (up to thousands of km^3) and associated hazard, the geomorphological and geotechnical characterization of large-scale sector collapses and related debris avalanche deposits attracted most of the attention of the scientific community (e.g., Apuani et al. 2005a; Moore et al. 1994; Urgeles et al. 1997; Deplus et al. 2001; Mitchell et al. 2002; Oehler et al. 2008; Del Potro and Hürlimann 2008; Romagnoli et al. 2009a, b; Coombs et al. 2007; Costa et al. 2014, 2015; Schaefer et al. 2015; Hildebrand et al. 2012, 2018). Conversely, the study of smaller landslides (up to few hundreds millions of m^3) was often

✉ Daniele Casalbore
daniele.casalbore@uniroma1.it

1 Institute of Environmental Geology and Geo-Engineering, National Research Council, Rome, Italy

2 Department of Structural and Geotechnical Engineering, Sapienza University, Rome, Italy

3 Department of Biological, Geological and Environmental Sciences, University of Bologna, Bologna, Italy

4 Department of Earth Sciences, Sapienza University, Rome, Italy

overlooked, especially in marine settings, due to the difficulties and time-consuming seafloor mapping of shallow-water areas around volcanic islands (Mitchell et al. 2008; Babonneau et al. 2013; Bosman et al. 2014; 2015,2018; Quartau et al. 2014; Sibrant et al. 2014; Casalbore et al. 2015). These landslides, if occurring in shallow-water or coastal sectors, can however generate local tsunamis, as recently observed at Stromboli in 2002 (Tinti et al. 2005) or Anak Krakatau in 2018 (Walter et al. 2019). Moreover, they can be more hazardous than the previous large events, due to their higher recurrence (e.g., Boudon et al. 2007; Di Roberto et al. 2010; Casalbore et al. 2012). In addition, turbidity currents generated from such landslides can pose a major hazard to offshore infrastructures (mainly subsea cables) that are critical for global communications and energy transmission (e.g., Carter et al. 2014; Talling 2014), especially in the case of small islands in developing countries (Clare et al. 2018).

The aim of this paper is to make an overview of small-scale landslides affecting the flanks of volcanic islands, with particular reference to their submarine part ("Overview of small-scale slope instabilities on volcanic edifices, with particular reference to their submarine flanks"). We use Stromboli volcano as a case-study for this kind of events, because several historical accounts of tsunami waves have been reported over the last two centuries (Maramai et al. 2005) and associated with speculated submarine landslides with mobilized volume in the order of millions of cubic meters. Most of them occurred within the Sciara del Fuoco (hereafter SdF, Fig. 1), a very steep subaerial-submarine collapse scar on the NW flank (Tibaldi 2001), which conveys towards the sea the volcaniclastic material produced by the persistent Strombolian activity at the summit craters (Kokelaar and Romagnoli 1995; Romagnoli et al. 2009a and reference therein). The accumulation and successive mobilization of large volumes of volcaniclastic deposits at SdF mainly occur during paroxysms or effusive eruptions which temporarily interrupt the persistent Strombolian activity and may affect the overall slope stability. This was, for instance, observed during the 2002 eruptive crisis, when two tsunamigenic landslides mobilized a volume in the order of ten million of m^3 both in the submarine and subaerial part of the SdF (Bonaccoro et al. 2003; Baldi et al. 2008; Chiocci et al. 2008a; Marani et al. 2008; 2009).

By combining high-resolution morpho-bathymetric monitoring of the SdF ("Small-scale slope instabilities at Stromboli: insights from morpho-bathymetric monitoring of Sciara del Fuoco") with slope stability analyses and results from previous studies ("Mechanisms controlling the development of small-scale submarine slope failures at Stromboli: a geotechnical perspective"), we attempt to better constrain the main triggering mechanisms for the development of submarine slope failures at Stromboli. Specifically, we analyze both the role of dyke intrusions (using as case-study the 2002 landslide) and the emplacement of lava flows and associated delta (using as case-study the 2007 eruption) on the stability of the submarine slope. Another possible trigger of small-scale landslides could be the entrance into the sea of pyroclastic flows, as those recently occurred in July and August 2019 at the Sciara del Fuoco. However, considering the paucity of information and modeling available in literature for this kind of events (apart from the paper of Freundt 2003), related geotechnical analysis is beyond the scope of this paper.

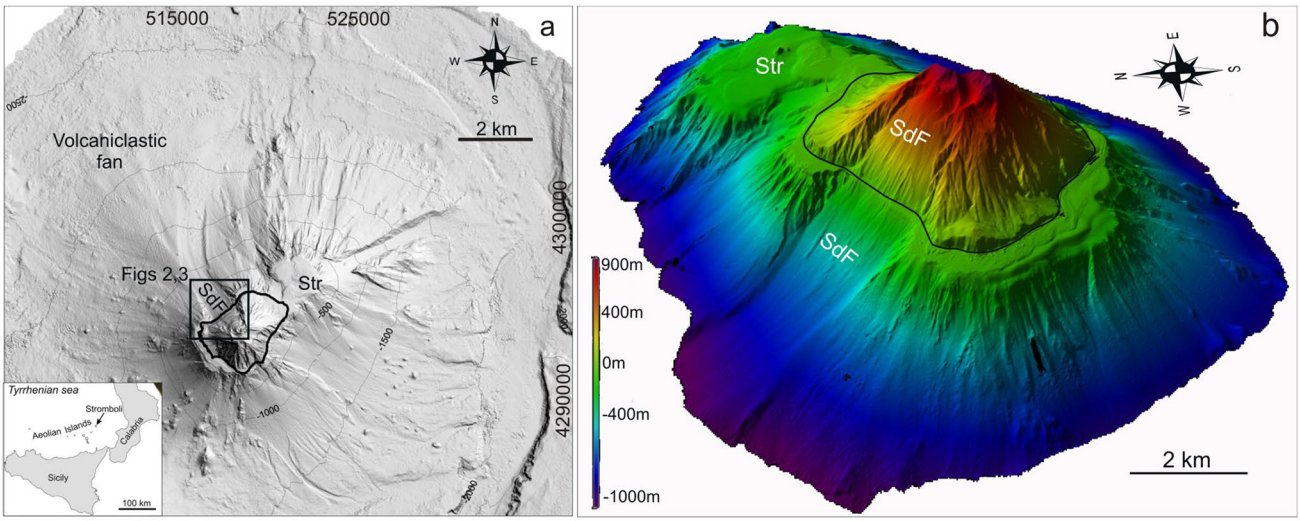

Fig. 1 **a** Shaded relief map of the Stromboli volcano (equidistance of isobaths: 500 m), elongated in a SW-NE axis; the coordinates are in WGS84-UTM33N; **b** 3-D view of the NW flank of Stromboli, featured by the submarine-subaerial scar of the Sciara del Fuoco (SdF) down to − 1000 m. *Str* Strombolicchio

Overview of small-scale slope instabilities on volcanic edifices, with particular reference to their submarine flanks

Volcanic edifices are some of the most rapidly growing geological structures on Earth. As a consequence, their flanks may become unstable and be subjected to failure at different temporal and spatial scale (Keating and McGuire 2000; McGuire 2003). The largest landslides (up to thousands of km^3) commonly affect oceanic shield volcanoes (e.g., Hawaii and Canary Islands, Mitchell et al. 2002), whereas smaller events (up to hundreds millions of m^3, typically in the order of millions of m^3 or less) are typically associated to steep stratovolcanoes or monogenetic cones. Stratovolcanoes are very prone to the development of shallow landslides, because of their structure made of layers of volcanic products with very different geomechanical and hydraulic characteristics (Madonia et al. 2019). Slope instability is also occasionally fostered where perched groundwater is sustained by horizons having low permeability (Chigira 2002). Moreover, volcanic soils may represent weak layers in the stratovolcano architecture, which highly increase landslide susceptibility at all spatial scales (Valadão 2002; Hurlimann et al. 2001).

In spite of their small mobilized volume, such slope instabilities can produce severe damages to the surrounding areas, both directly and indirectly. Direct risk occurs when inhabited areas are located within the runout distance of the debris flow/avalanche generated by the landslide. This is for instance demonstrated by the earthquake-triggered Las Colinas landslide, a 180,000 m^3, fast-moving flow-like landslides occurred in 2001 at El Salvador (Central America), resulting in about 500 casualties (Crosta et al. 2005; Devoli et al. 2009). In volcanic islands, it should be considered that inhabited areas are often built close to active volcanoes with noticeable landslide hazard, as for instance observed at Vulcano Island in Italy (Galderisi et al. 2013; Marsella et al. 2013). Moreover, runout distances can be larger for volcanic landslides, as they are typically characterized by a higher mobility than those involving non-volcanic rocks; this mobility generally increases with the volume of the landslide (Hayashi and Self 1992; Legros 2002). Indirect risks are associated with the generation of tsunami waves when volcanic landslides enter into the sea or a lake. For instance, the tsunamis waves generated by the 2018 Anak Krakatau slope failure mobilizing a subaerial volume of 100–400 million of m^3 (Walter et al. 2019; Williams et al. 2019), caused over 430 fatalities and14,000 injured people along the Sunda Strait.

Since their volume is not extremely large (on average around few millions of m^3) and volcanic flank are often steep, the recurrence time for "small-scale" volcanic landslides is quite short (especially if compared to that of large-scale sector collapses). This is witnessed by several historical examples reported in literature, such as Montserrat in 2000 (Sparks et al. 2002), Stromboli in 2002 (Bonaccorso et al. 2003; Chiocci et al. 2008a), Mount Meager in 2009 (Guthrie et al. 2012), Askja in 2014 (De Vries and Davies 2015) and Anak Krakatau in 2018 (Walter et al. 2019). Historic accounts reveal that only in Southeast Asia, 17 volcano-induced tsunamis have been recorded during the twentieth century and (at least) 14 in the nineteenth century, thus defining a recurrence rate of one event every 5–8 years (Paris et al. 2014).

Monitoring of 2018 Anak Krakatau slope failure revealed that at the time of the collapse, none of the triggering factors, including the thermal anomalies, flank motion, anomalous degassing, seismicity, and infrasound data, was sufficiently conclusive to shed light on the failure if considered individually (Walter et al. 2019). This example demonstrates how, once stability conditions have progressively worsened throughout years before the event, specific (and sometimes minor) internal and external perturbations can trigger a collapse. This is consistent with the evidence that volcanic edifices are by their nature "unstable" systems due to structural discontinuities, hydrothermal alteration, magmatic intrusions and high lava accumulation rates (de Vries and Davies 2015). Specifically, different predisposing/triggering mechanisms have been proposed for the development of small-scale, subaerial landslides, such as:

a. heavy rainfall can be considered in humid areas as one of the principal triggering events influencing the distribution, frequency and magnitude of landslides on volcanic slopes, as for instance observed in the Azores islands (Valadao et al. 2002);
b. Loading of an active dome over a weak, hydrothermally altered slope in arc-volcanic settings, as for instance occurred at Monserrat (e.g. Sparks et al. 2002);
c. Seismic action and surface faulting involving the volcano edifice that may trigger failure, as at Iriga Volcano in Philippines (e.g. Paguican et al. 2012);
d. Shallow hydrothermal fluids that can stagnate under subhorizontal surfaces, giving rise to the argillification of volcanogenic minerals (Madonia et al. 2019; Olivares and Tommasi 2008). Fumarolized areas are particularly prone to gravitational instability, and critical conditions can be reached after rainfall, as testified by the several shallow landslides affecting La Fossa cone (Vulcano Island) in the last three decades (Madonia et al. 2019);
e. Deep glacial incisions and glacial retreat can erode and debuttress a volcanic edifice lying in alpine chains or at high latitudes, producing steep slopes that are prone to frequent landslides (especially if the edifice was already

weakened by hydrothermal alteration) as observed at Mount Meager in 2009 (Guthrie et al. 2012);

f. Vertical movements associated with caldera resurgence, as testified by the widespread mass-transport deposits (often entering into the sea) sourced from the rapid uplift of the Mt. Epomeo (Ischia island) in the past 30 ka (Tibaldi and Vezzoli 2004; De Vita et al. 2006).

Regarding submarine volcanic flanks, a main problem for the event reconstruction is the paucity of observation or monitoring of landslides due to the technological and logistical difficulties related to the water column. Until now, seafloor imagery systems (i.e., multibeam and side scan sonar systems) coupled with high-resolution seismic profiles (even if these often do not work very well on the steep and coarse-grained volcanic flanks) have been used to map the extent and spatial distribution of the geomorphic features associated with past landslides. Particularly, seafloor mapping around volcanic edifices has allowed the identification of wide debris avalanche deposits associated with large-sector collapses in the subaerial/submarine flanks of volcanic edifices (e.g., Mitchell et al. 2002; Boudon et al. 2007; Coombs et al. 2007; Leat et al. 2010), but also widespread landslide scars associated to small-scale events. These landslide scars have typically widths of hundreds- or thousands of meters and are commonly recognized at the edge of the insular shelf surrounding volcanic islands at water depths around 100–200 m, as observed in the Azores (Quartau et al. 2010, 2012; Casalbore et al. 2015), Madeira Archipelago (Quartau et al. 2018; Santos et al. 2019), Aeolian Islands (Casalbore et al. 2011, 2016a; Romagnoli et al. 2013) and Ventotene Island (Casalbore et al. 2016b). The insular shelf edge marks, in fact, the passage from a gently sloping area carved by wave-erosion during sea-level fluctuations to the steep volcanic flanks, where slope gradients reach values higher than 30°. In the shelf area, there may be also the temporary storage of loose volcaniclastic sediments eroded from the coast and transported seaward during the main storm-surges, which can be successively remobilized at higher depths by slope failures (Meireles et al. 2013; Casalbore et al. 2017).

In the submarine volcanic flanks where the shelf is lacking or retrogressive erosion at the head of canyons/channels/gullies is very strong, landslide scars are found in very shallow water (5–20 m water depth) and close to the coast (to a distance of few tens of meters), thus suggesting the occurrence of a main geohazard for coastal communities. This is, for instance, observed on the eastern side of Lipari (Casalbore et al. 2018), within the submarine part of La Fossa Caldera at Vulcano (Romagnoli et al. 2012) or at Tanna Vulcano (Clare et al. 2018). In all the presented cases, landslide deposits are difficult to recognize on multibeam bathymetry. This is likely due to the fact that landslide masses lost cohesion either during failure or during its runout, evolving in a sedimentary gravity flow (i.e., turbidity currents).

The detection of recent landsliding events in marine setting is possible through the comparison of repeated multibeam surveys or with acoustic monitoring system so far. Repeated multibeam surveys performed at Monowai Volcano in the Kermadec arc allowed the identification of two small-scale landslides between 200 and 800 m water depth (Chadwick Jr et al. 2008). Both slope failures have been interpreted by these Authors as the result of loading of volcaniclastic material erupted in the last 30 years on the summit and on the steep upper slopes of the submarine volcano (> 20°). The thicknesses (48–70 m) and volumes (40–85 million of m^3) of the landslides at Monowai are very similar to those depicted at NW Rota-1 Volcano in the Mariana volcanic arc (Chadwick et al. 2012), thus suggesting that this size of the event may be typical of young, active submarine arc volcanoes. This conclusion is also supported by analogue experiments conducted to investigate the modes of sector collapse on volcanoes, showing that shallow and narrow collapses are a common mode of failure at the summit of steep-sided cones (Acocella 2005).

Acoustic monitoring records the signals released by landslides either through hydrophones or, if the signal couples into the ground, seismometers. This monitoring system has been largely applied to subaerial volcanoes (Allstadt et al. 2018 and reference therein). In the submarine environment, the deployment of hydrophone on the summit of Loihi volcano in 1998 allowed to recognize dozens of small landsides occurring on the submarine flank of Kilauea (Caplan-Auerbach et al. 2001). Particularly, these events were recorded only when lava was actively flowing into the ocean, suggesting that landslides were triggered by loading of new material at the top of a marginally stable flank (Caplan-Auerbach et al. 2001). A similar approach was successfully applied also at the NW Rota-1 (Chadwick et al. 2012) and West Mata volcano in the Lau Basin (Caplan-Auerbach et al. 2014).

Data and methods

The review of submarine slope instabilities along the Sciara del Fuoco at Stromboli is largely based on time-lapse morpho-bathymetric data collected in the area since 2002. They were used both to reconstruct the morphological evolution of the slope and, coupled to geotechnical properties of volcaniclastic materials and strength/stiffness estimates of the lava flow rock mass, to investigate triggering mechanisms in the volcaniclastic slope and in the slope area overlaid by the 2007 lava delta, respectively. Several bathymetric surveys were collected since 2002 with multibeam systems operating at different frequencies (50–455 kHz) on board

of RVs *Thetis*, *Urania* and *Minerva Uno* (CNR) and of small launches for coastal surveys. Bathymetric data were positioned through differential GPS systems and processed with *Caris Hips and Sips* hydrographic software with the application of tidal correction, sound velocity profiles, patch test, statistical/geometrical filters and manual editing (for details on data acquisition and processing, a reader can refer to Baldi et al. 2008; Bosman et al. 2014, 2015). Once processed, raw data were gridded and used to generate Digital Elevation Models (DEMs) of the seafloor with cell size variable from 0.5 to 3 m according to sounding density in the different depth range. Seafloor changes were computed as the difference between two successive DEMs generated from repeated multibeam surveys. The resulting "difference maps" quantify the change in seabed depth, where positive and negative values are associated with seafloor accretion and erosion, respectively. The volumes associated with surface changes are obtained by integrating the difference in depth over the area of interest through Global Mapper 16 dedicated to the calculation of volumes. The reliability of computed volumes depends on the accuracy of the DEMs, which, in turn, is related to uncertainties in seafloor depth estimation. Several source of errors can affect the accuracy of the soundings data, such as the system used in surveys (frequency and beam width), measurements of acoustic wave velocity in the water, offset of the vessel configuration, calibration procedures, accuracy of positioning (PPK, RTK, HP, EGNOSS, etc.), tidal correction and so on. Small depth changes below the likely errors in the DEMs, are not taken into account in volume computations. As threshold it was assumed ± 1 m, defined by comparing the difference in depth of stable benchmarks between pairs of successive bathymetric sets.

The influence of dyke intrusion and deposition of the 2007 lava delta have been analyzed through stress–strain finite difference analyses (FLAC and FLAC3D codes). Physical and mechanical properties of the volcaniclastic materials used in the model are based on the results of comprehensive laboratory tests reported in previous studies (Verrucci et al. 2019; Rotonda et al. 2010; Boldini et al. 2009; Tommasi et al. 2005). The estimate of the strength and stiffness assumed for the rock mass forming the lava delta is based on laboratory tests conducted on the subaerial lava flows by Rotonda et al. (2010) and data on rock mass structure collected during scuba surveys of the submarine scarps of the lava flow.

Geological setting

Stromboli is one of the seven islands forming the emerged part of the 200 km-wide Aeolian volcanic arc in the Southern Tyrrhenian Sea. Particularly, Stromboli Island is the tip (around the 2%; Bosman et al. 2009) of a large and mostly basaltic stratovolcano that rises over 3000 m from the surrounding seafloor (Fig. 1). The stratovolcano is actually made up by two volcanic edifices: (1) the older edifice (Str in Fig. 1), largely eroded and completely submerged apart from the central neck of Strombolicchio, which is dated around 200 ka (Gillot and Keller 1993), and (2) the younger Stromboli edifice forming the present-day island, dated around 85 ka on the base of the oldest outcropping rocks (Francalanci et al. 2013).

The Stromboli edifice is characterized by a bilateral symmetry with respect to a SW–NE axis, with the SE and NW flanks repeatedly affected by large lateral collapses (Romagnoli et al. 2009a, b; Tibaldi et al. 2009). In detail, the NW flank was affected by multiple sector collapses in the last 13 ka (Tibaldi 2001), the last of them likely occurred during medieval times, leading to the development of the Sciara del Fuoco scar (Francalanci et al. 2013). Geoarchaeological evidence of Middle-Age tsunamis at Stromboli have been recently reported by Rosi et al. (2019).

The volcanic activity of Stromboli is mostly characterized by the so-called "normal Strombolian activity" (or persistent ordinary activity), consisting of low- to mid-energy Strombolian explosions and the continuous emission of volcanic gases (Barberi et al. 1993; Bertagnini et al. 2003). A second type of explosions, named Strombolian paroxysms (Mercalli 1907), consists of short-live violent explosions involving more than one vent. These can further be subdivided into small-scale paroxysms (Barberi et al. 1993; Métrich et al. 2005), and large-scale paroxysms, often called "Paroxysms" for simplicity (Bertagnini et al. 2011), as recently occurred in July and August 2019. Finally there are rare lava flow emissions within the SdF, as recently occurred in 2002, 2007 and 2014 (Calvari et al. 2005, 2010; Di Traglia et al. 2018a). Most part of the erupted volcanic material is funneled within the SdF scar into the sea, where a large volcaniclastic fan, formed by debris avalanche deposits and an overlying turbidite system, is recognizable from about − 700 m down to − 3000 m (Romagnoli et al. 2009a; Fig. 1). The volcaniclastic fan extends over an area of 170 km^2 for a total estimated volume of 12 ± 2.5 km^3. Grabs and box-corers, performed off the SdF submarine scar, recovered Stromboli-derived turbidites with very coarse sand and small basalt pebbles at water depths greater than 2000 m, indicating a considerable bypassing of finer sediments by long-lived and strong surging currents towards the SE Tyrrhenian bathyal plain (Kokelaar and Romagnoli 1995; Lucchi and Kidd 1998; Marani et al. 2008, 2009; Romagnoli et al. 2009a; Di Roberto et al. 2010).

Small-scale slope instabilities at Stromboli: insights from morpho-bathymetric monitoring of Sciara del Fuoco

The 2002 tsunamigenic landslide

On December 30th, 2002 a submarine-subaerial sequence of landslides affected the NE-most portion of the Sciara del Fuoco, generating two tsunami waves with a run-up of 2–10 m on the Stromboli coasts (Bonaccorso et al. 2003; Tinti et al. 2005, 2006). The geometry of the submarine landslide scar was reconstructed using the difference map (Fig. 2) obtained through the comparison of bathymetries collected before (February 2002) and after (January 2003) the 2002 event (landslide T in Fig. 2a; Chiocci et al. 2008a). The landslide scar developed from the coast down to − 350 m, with a length of 650 m, width of 470 m and a maximum thickness of 45 m. The landslide mobilized an estimated volume of approximately 11×10^6 m^3 of volcaniclastic materials and lava (Baldi et al. 2008). The submarine landslide scar t caused 7 min later two subaerial landslides (β plus γ landslides in Fig. 2a; Tommasi et al. 2005), having a total volume of approximately 13.5×10^6 m^3 (Baldi et al. 2008).

The submarine and subaerial tsunamigenic landslides were caused by larger, deep-seated gravitational slope deformations (landslide α of Tommasi et al. 2005, 2008) triggered by the emplacement of a SW–NE dyke during the 2002–2003 eruption (Bonaccorso et al. 2003; Calvari et al. 2005), as discussed in more detail in the next sections. The morphological setting of the submarine slope strongly controlled the development of the landslide scar as it mainly affected the shallower and steeper part (gradients > 30°, up to 40°, Fig. 2b; Casalbore et al. 2011), where a volcaniclastic apron develops down to 300 m of depth, made up by the coalescence of several fan-shaped bodies, in morphological continuity with similar features observed on the lower subaerial slope of the SdF (Fig. 1b; Chiocci et al. 2008a).

Grabs in this area recovered coarse sand, centimetric to decametric scoriae and vesicular lava pebbles, whereas finer fractions were very low or totally absent (Casalbore et al. 2010). This suggests that volcaniclastic fine sand mainly bypassed this sector and/or was removed from the submarine SdF, likely by frequent small submarine slope failures and by severe storms that struck the NW flank of Stromboli during winter months, and related northward-directed littoral

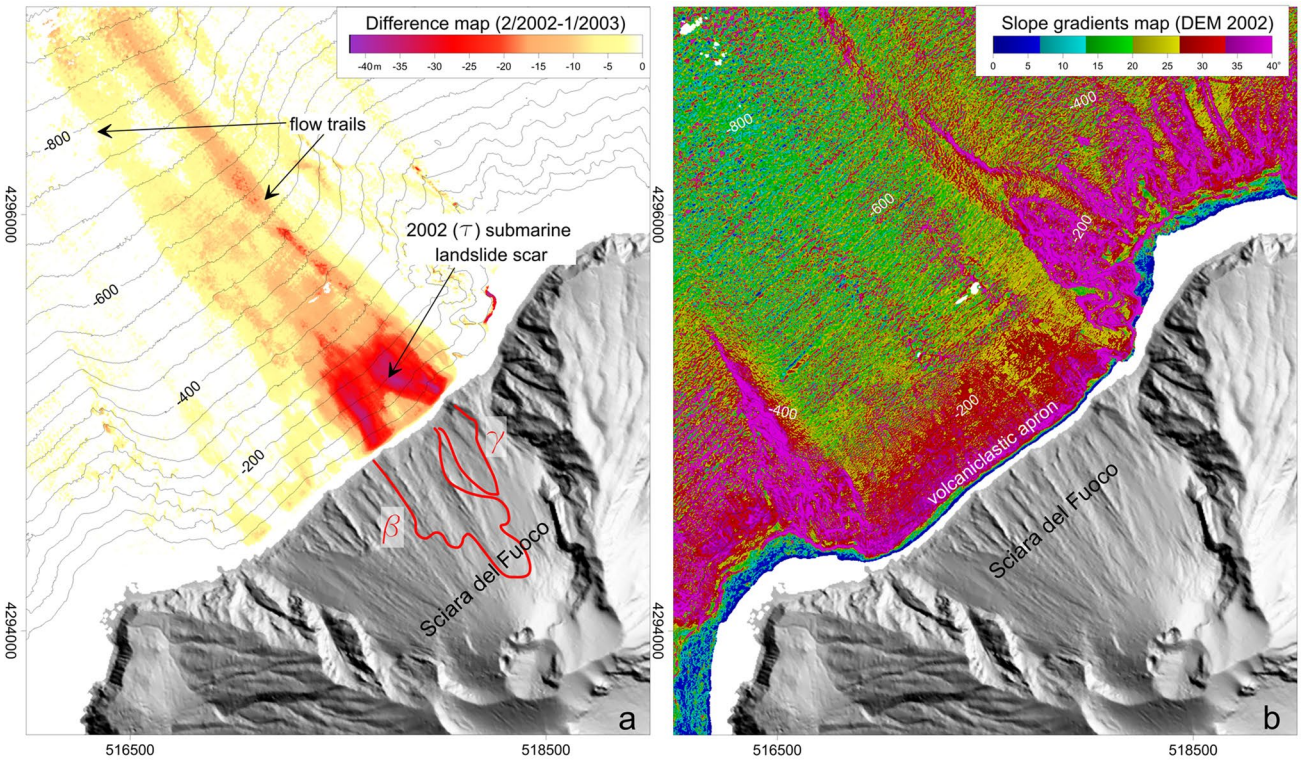

Fig. 2 **a** Difference map obtained by comparing multibeam bathymetries acquired pre- (February 2002) and post-slide (January 2003) showing the geometry of the 30th December 2002 submarine scar down to—350 m; at greater depths two flow trails, associated to the erosion exerted on the seafloor by the sliding mass, are also recognizable; **b** Slope map (in degrees) computed on the pre- (February 2002) slide DEM, indicating a steeper part of the submarine slope (volcaniclastic apron) in the first 300 m of depth

drift as suggested by Romagnoli et al. (2006). This inference is also suggested by the sedimentological studies performed on the 2002 landslide deposits, found at depths ranging between 1000 and 1800 m, through the integration of multibeam bathymetry, side-scan sonar and seafloor visual observations (Marani et al. 2008, 2009). Characteristics of the deposits suggest that they were derived from cohesionless density flows with sandy matrix. Flow rheology and dynamics led to the segregation of the density flow into sand-rich and clast-rich regions. Proximal coarser landslide deposit were found on the volcano slope, while a distal, cogenetic, sandy turbidite was observed 24 km far from the Stromboli shoreline (Marani et al. 2008, 2009), indicating a prevalent by-pass of the sedimentary gravity flows.

Emplacement of the 2007 lava delta and its successive morpho-bathymetric evolution

The post-slide evolution of the 2002 submarine landslide scar was monitored through repeated bathymetric surveys, evidencing its rapid infilling (approximately 40%) over a period of only 4 years after the event (Chiocci et al. 2008b). At the beginning of 2007 a new effusive eruption emplaced between 3.2×10 and 11×10 million of m^3 of lava on the NE sector of the SdF (Calvari et al. 2010), most of which on the submarine slope (approximately 70% according to Bosman et al. 2014). The difference map obtained between multibeam surveys collected before and after the 2007 eruption allows us to constrain the geometry and volume of the submarine portion of the lava delta (Fig. 3a).

This extended down to −600 m, with a maximum thickness of 65 m (on average 50 m) and covered an area of 420×10^3 m^2, most of which within the 2002 landslide scar, which was already almost filled by volcaniclastic material funneled into the SdF (Fig. 3). It is noteworthy that very small-scale landslides occurred also during the emplacement of the lava delta, as testified by the slope failure recognized in the 17-h delay (5–6 of March 2007) difference map. They mobilized a volume of about 30 thousands of m^3 (Bosman et al. 2014).

Repeated bathymetric surveys were performed after the emplacement of the 2007 lava delta to monitor the evolution of the submarine slope, showing a relatively slow and gradual dismantling of the upper part of the lava delta (mainly in the first 100 m of depth) through small and shallow failures. The cumulative seafloor erosion associated with these

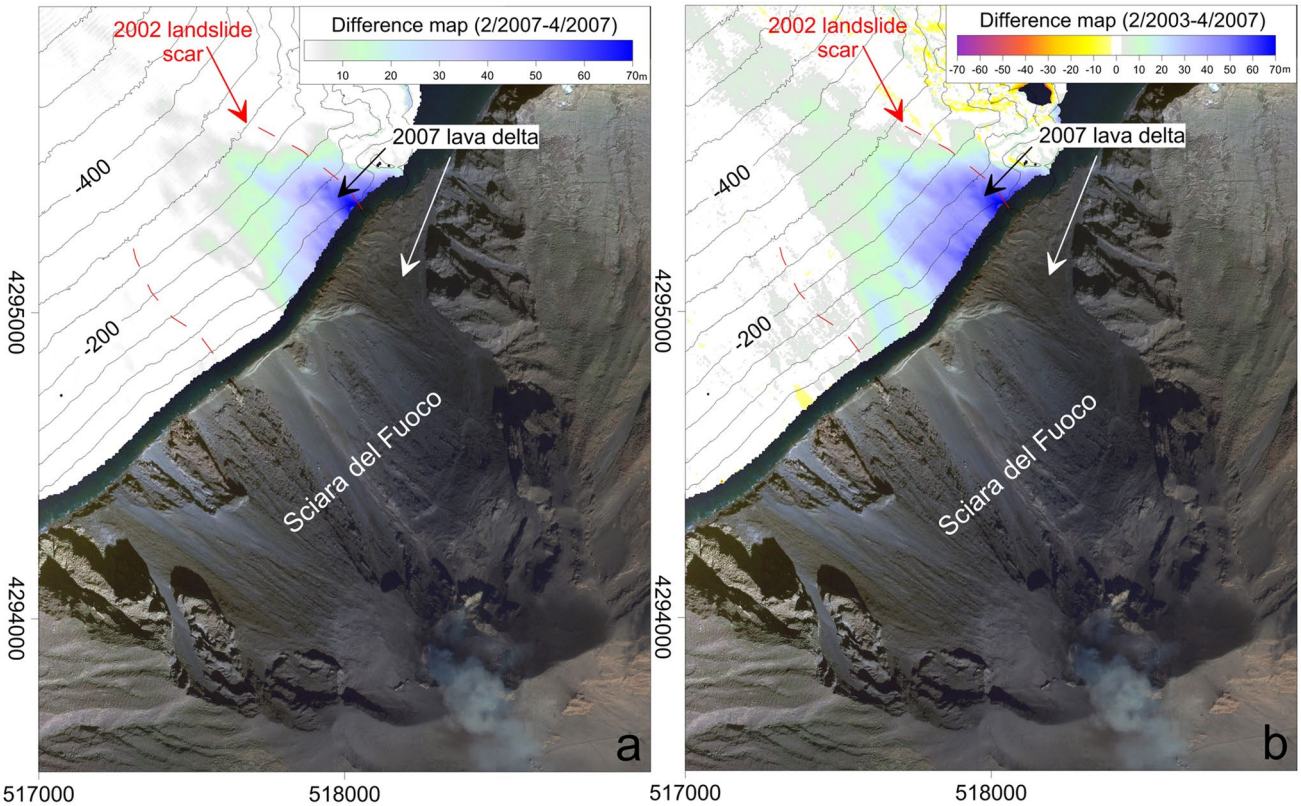

Fig. 3 **a** Difference map computed by comparing pre- (February 2007) and post- lava delta emplacement (April 2007) multibeam bathymetries, evidencing the associated seafloor accretion; **b** Difference map computed by comparing multibeam bathymetries acquired in January 2003 and April 2007, showing the almost complete filling of the 30th December 2002 scar

shallow slope failures during the period 2007–2013 is shown in the difference map of Fig. 4. Seafloor erosion mainly occurs down to − 150 m and is mostly confined within the part of the lava delta emplaced within the 2002 landslide scar. The thickness of the mobilized material from the lava delta varies between 4 and 14 m, yielding a total estimated volume of approximately 500 thousands of m^3. This value is underestimated because it is limited to a water depth > 20 m (limit of the bathymetric survey) and can partially include material coming from the frequent avalanches that occurred on the subaerial slope. Deposits (positive bathymetric residuals) associated to submarine erosion and slope failures are found between 200 and 400 m water depth, accounting for more than 1 million of m^3.

Mechanisms controlling the development of small-scale submarine slope failures at Stromboli: a geotechnical perspective

The recent history of the SdF has indicated that small-scale instability phenomena in the submarine slope (i.e. the 2002 tsunamigenic landslides, "The 2002 tsunamigenic landslide") involve only the volcaniclastic material that infills the scar and are triggered by both internal and external loads, i.e. magma pressure and accumulation of eruptive products, respectively.

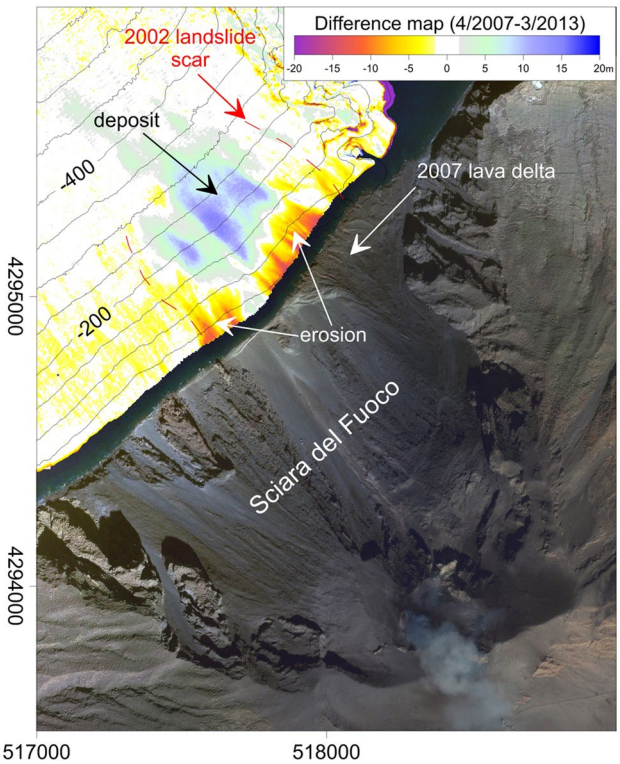

Fig. 4 Difference map obtained by comparing the multibeam bathymetries collected in April 2007 and March 2013, showing that erosive processes mainly affected the shallower part (down to about − 100/− 150 m) of the submarine lava delta, while deposits are recognizable downslope

However, stress/strain increments require that specific conditions are established in the submarine slope to trigger instability phenomena. In fact, the shear strength of all volcaniclastic materials forming the most part of the SdF infilling is relatively high to ensure stability of the submarine slope in drained conditions, i.e. when the stress/strain rate is not large enough to induce excess pore pressures in the saturated material forming the submarine slope (Rotonda et al. 2009; Verrucci et al. 2019). Conversely, if stress/strain rates are as high as to induce significant excess pore pressures (i.e. to establish undrained conditions) a static liquefaction mechanism can develop and the allowable shear strength is greatly reduced. The "threshold" of the stress/strain rate that marks the limit between drained and undrained behavior is very high because the hydraulic conductivity of the volcaniclastic material is high, thus allowing rapid dissipation of excess pore pressures. In this respect, triaxial tests conducted on both the coarser and more abundant (gravel) and the finer (sand) component of the volcaniclastic material indicated that only the latter is susceptible to reach static liquefaction (Tommasi et al. 2016).

As mentioned in the introduction, different phenomena can modify the state of stress/strain in the submarine slope (Fig. 5): (I) dyke intrusions; (II) emplacement of lava flows into the sea and associated lava delta, (III) pyroclastic flows (not discussed in this paper). At Stromboli, dyke intrusions, lava flows and pyroclastic flows are associated with paroxysmal or effusive eruptions that temporally interrupt the "normal" Strombolian activity. In addition, Di Traglia et al. (2018b) indicate that seismic shaking can trigger slope instability both at shallower and deeper levels, as previously suggested by Voight and Elsworth (1997).

Despite dyke intrusion commonly occurs in the proximity of the alimentation conduit (i.e. mainly in the uppermost one third of the emerged portion of the SdF), 3D finite-difference stress–strain numerical analyses (Casagli et al. 2009; Verrucci et al. 2019) indicate that this process can induce significant shear strains down to the near-shore zone of the submarine slope (Fig. 6), under conditions that have already occurred in the past (December 2002). Lava flows have often extended down to the submarine slope of SdF (Marsella et al. 2012) and may apply significant vertical loads over wide areas, e.g. as it occurred during the 2007 eruption, when a lava delta extended over 4.2×10^5 m^2 with a maximum thickness of 65 m ("Emplacement of the 2007 lava delta and its successive morpho-bathymetric evolution" and Fig. 3a). Pyroclastic flows entering the sea can load the seafloor according to different mechanisms, also depending on the density and temperature of the flowing/avalanching

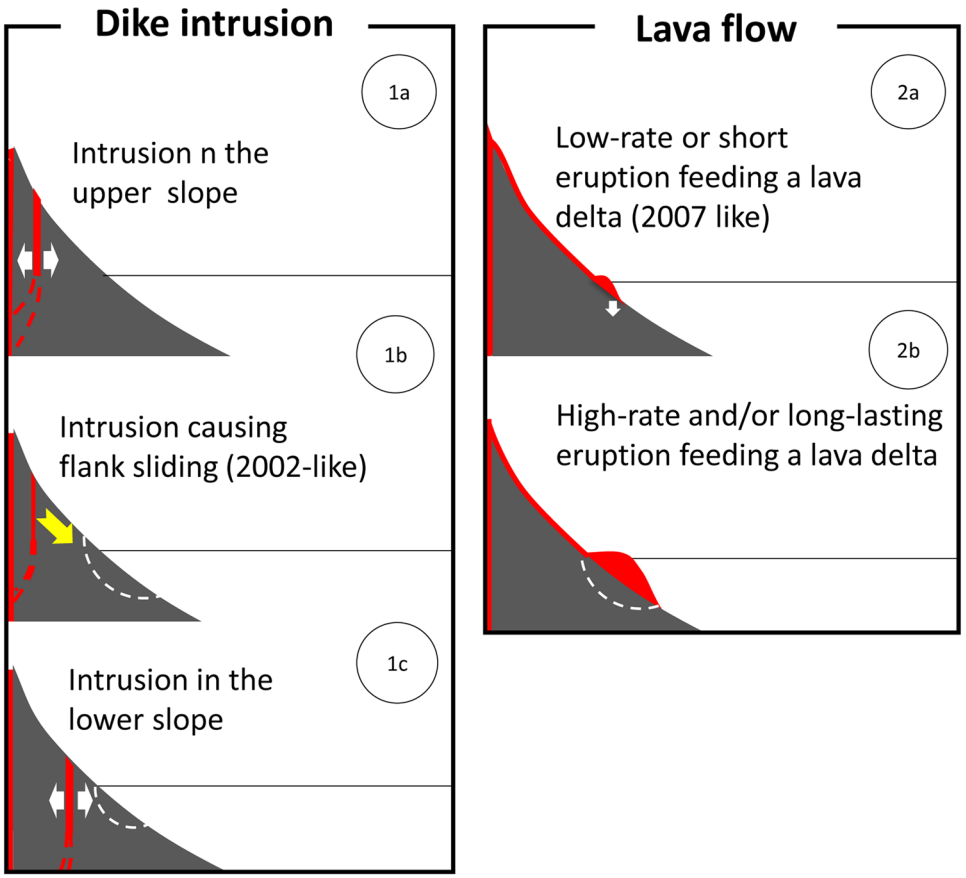

Fig. 5 Sketch of the main mechanisms that can potentially trigger submarine slope failures on the SdF slope (for more details see the main text)

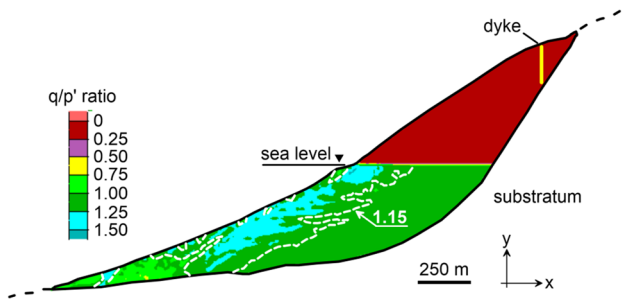

Fig. 6 Distribution of q/p' values within the modelled subaerial and submarine part of the SdF slope

mass (3a and b in Fig. 5; see Voight et al. 2012; Freundt 2003; Hart et al. 2004; Trofimovs et al. 2006, 2012). The most recent events were observed immediately after the July 3rd and August 28th, 2019 paroxysms (https://lgs.geo.unifi.it/index.php/reports/stromboli-daily), but these phenomena are quite frequently reported at Stromboli (Calvari et al. 2006; Rosi et al. 2006; Pistolesi et al. 2008, 2011; Bertagnini et al. 2011; Andronico et al. 2013; Di Roberto et al. 2014; Salvatici et al. 2016). In the following section, the mechanisms that can occur in the first two loading conditions (diking and lava overloading) are discussed based on data acquired during more than 10 years and the results of numerical models of the submarine slope.

Dyke intrusion (scenario like the 2002 submarine landslide)

The rate of stress/strain induced by dyke intrusion (1a in Fig. 5) is relatively low in comparison to that required to establish undrained conditions. Nevertheless, observations preceding the 2002 failures (Tommasi et al. 2008) clearly showed that deformations can localize along shear surfaces extending down to the submarine slope (1b in Fig. 5). Under these conditions, deformations occur at higher rate and can experience sudden accelerations. In the submarine slope, if strain acceleration is sufficiently high, the induced excess pore pressures are not readily dissipated, i.e. undrained conditions are established. For a contractive soil, excess pore pressures are increased (Boldini et al. 2009) and, in turn, induce further plastic strain through a self-sustaining process driving towards a runaway extensive failure, i.e. liquefaction. Local strain accelerations can be induced, for instance, by stress accumulation and subsequent sudden failure of more resistant parts (even small) that are inevitably included within such an inhomogeneous deposit (1b in Fig. 5).

Numerical analyses performed since 2003 demonstrated that the three-dimensional nature of the SdF slope significantly influences the amount of internal forces (as, for example, the magma thrust) needed to reach a certain strain level (Apuani et al. 2005b; Apuani and Corazzato 2009; Casagli et al. 2009; Marsella et al. 2009; Verrucci et al. 2019). Nevertheless, the main aspects of the loading and deformation patterns can be observed also in less time-costing, two-dimensional analyses.

A novel numerical model has been set up to analyze stress and strain distribution in the submarine slope. Plane-strain (2D) numerical analyses have been performed along a profile centered on the SdF (Fig. 6) again through an explicit finite difference code (FLAC; Itasca 2011). Analyses have also provided an accurate computation of the stress ratio q/p' between the deviator stress and the mean effective stress, which characterizes the local mobilization of the shear strength in mean pressure-sensitive materials as the coarse-grained soils forming the submarine slope. The model has a vertical extension of 1240 m (between elevations − 610 m and + 630 m) and a horizontal extension of 2800 m, 1600 of which over the offshore part of the volcano flank. The model was discretized into isometric quadrangular elements with a side length of 10 m. The finite difference analysis models only the volcaniclastic infilling of the SdF. A boundary condition with fixed grid points is imposed at the model bottom, along the contact with the stiffer and stronger rock substratum (as deduced from Kokelaar and Romagnoli 1995). A hydrostatic distribution is applied as both a mechanical pressure onto the seafloor and a pore-water pressure in the material located at elevations lower than the sea level (dry conditions are assumed above the sea level). The volcaniclastic infilling of the SdF was schematized as a continuum but it was assigned the *ubiquitous joint model* (UJM) to account for the presence of thin and continuous sandy horizons (parallel to the slope) within the coarser (gravel and cobbles) volcaniclastic deposit. The UJM (Itasca 2011) is an elastic-perfectly plastic constitutive model with two distinct yield criteria. One for the material "matrix" and one for a weak ubiquitous plane at a given inclination to the horizontal plane. The matrix (i.e. the coarse volcaniclastic material) is assigned a Mohr–Coulomb bi-linear criterion (with parameters c'_1, φ'_1 and c'_2, φ'_2 acting at low and high normal stress, respectively), which accounts for the non-linear confinement-dependent strength of coarser volcaniclastic material. The four parameters were determined through large-size direct shear tests. A linear criterion was assumed along the orientation of the weak horizons with strength parameters c'_j, φ'_j, determined through Bishop ring shear tests. Mechanical properties are summarized in Table 1.

The stress distribution was calculated simulating a gradual "deposition" of layers parallel to the sub-aerial slope. Differently from the previous analyses, the layer thickness was reduced to about 100 m (the height of ten rows of elements) in order to increase the continuity of the stress path. In addition, the bulk density, ρ_d, and the elastic constants (Young E modulus and shear modulus G) were gradually increased with the mean stress (i.e., with depth) during the deposition, according to the results of a large-size oedometer compression test reported by Tommasi et al. (2005). This procedure yields a more accurate distribution of the internal stresses of the deposit, which is fundamental for assessing the original "distance" of the current state of stress from failure conditions and the effect of successive stress changes.

At the end of the "deposition" stage of the analyses, large part of the submarine slope, down to -200 m (up to 750 m offshore) reaches values of q/p' higher than 1.15 (Fig. 6), i.e. the threshold for the occurrence of flow liquefaction in the finer volcaniclastic material, identified in K_0-consolidated undrained triaxial tests (Verrucci et al. 2019). Dimensions of the potential landslide depend on the extent and continuity of sandy horizons. In fact, finer materials are the sole, within the volcaniclastic apron forming the submarine Sciara del Fuoco down to − 300 m, that can experience liquefaction (Verrucci et al. 2019). Sandy layers have not necessarily to form the whole or most of the failure surface, but the dramatic drop of shear strength at liquefaction has to involve one or more layers that should extend enough to propagate failure also within the surrounding coarser materials forming most of the volcaniclastic apron. The possible activation of the liquefaction phenomenon is strictly subordinated to the fact that a relevant stress increment occurs in undrained conditions and the void ratio is sufficiently high to let the material contract in response to stress changes. There is a poor likelihood that all required conditions verify within the whole SdF slope with high stress ratios. Nevertheless, this q/p' distribution gives some clues about the most conservative scenario of a failure controlled by a liquefaction mechanism.

Table 1 Geotechnical properties of the volcaniclastic materials utilized in the numerical model. For mean-stress-sensitive properties, extreme values over the p' range are shown

	ρ_d Mg/m^3	E GPa	G GPa	c'_1 kPa	φ'_1 °	c'_2 kPa	φ'_2 °	c'_j kPa	φ'_j °
Min p' (0.8 MPa)	1.55	0.65	0.25	5	44	335	26	0	36
Max p' (6 MPa)	2.05	4.03	1.55	5	44	335	26	0	36

The analyses performed by Verrucci et al. (2019) show that the stress ratio distribution in the submarine slope is not altered by a lateral dyke introduced in the 2D section at an elevation of about 620 m, as observed in the field by Acocella et al. (2006), Casagli et al. (2009), and Di Traglia et al. (2018c, 2018d) for the 2002–2003, 2007 and 2014 flank eruptions, respectively. A dyke-induced thrust exceeding 10 kPa/m produces within the subaerial slope a shear band at the toe, which crops out about at the shoreline; i.e. the magma thrust is dissipated through a sliding plastic mechanism before further stress adjustments propagate down to the submarine slope. Actually, a dyke intrusion can directly activate significant movements in the submarine portion only if branches down to low elevation (1c in Fig. 5) as evidences from recent eruptions suggest. This result supports the consideration that volcanic activity can trigger major submarine failures only through a more complex indirect process as that previously discussed.

Lava flows entering the sea and associated delta

The effect of a lava delta on the stability of the submarine slope was modelled on the lava delta built by the 2007 eruption and reconstructed through high-resolution bathymetries and observations from scuba dives (Bosman et al. 2014). The lava body in the 2D section is representative of the geometry of the lava-delta in its central area. It is strip-shaped with a maximum thickness of about 65 m and extends horizontally 200 m uphill from the shoreline and 500 m off the shoreline over the submerged slope (Fig. 7, inset). Geotechnical properties adopted for the lava delta are reported in Table 2.

The rock mass was assigned a Mohr–Coulomb strength criterion whose parameters c_b and φ_b were obtained by linearizing the Hoek–Brown strength criterion (HB), through the procedure proposed by Hoek et al. (2002). The HB parameters of the rock mass were calculated from the strength parameters (m_i and σ_{ci}) of subaerial lava specimens determined by Rotonda et al. (2010), and from the GSI index (Marinos et al. 2005) estimated from data collected during scuba surveys. GSI values may range from 35 to 50, depending on the lava flow structure; the lower GSI value was chosen in our case to model a more conservative scenario. The choice of the HB criterion for the rock mass is supported by the irregular and intense fracturing observed on the scarps of the lava delta. The deformability of the rock mass was estimated, based on the GSI value, according to Hoek et al. (2002).

The delta accretion was simulated through the addition of 10-m-wide vertical slices in downslope direction. The results show that the effect of the increasing load applied by the lava delta is not sufficient to cause instability, but it induces a field of displacements, localized within the delta itself and in few tens of meters of the underlying volcaniclastic deposit (Fig. 7). The maximum displacements occur on top of the lava delta after completion of the accretion process (over 1.4 and 2.2 m in the vertical and horizontal component, respectively). Waving values of the displacements along the lava delta are related to the numerical procedure of accretion simulation, that is unavoidably discontinuous.

These results agree with the slow and progressive dismantling observed for the 2007 lava delta until the 2013 (Fig. 4), where small slope failures affected the upper (< − 150 m)

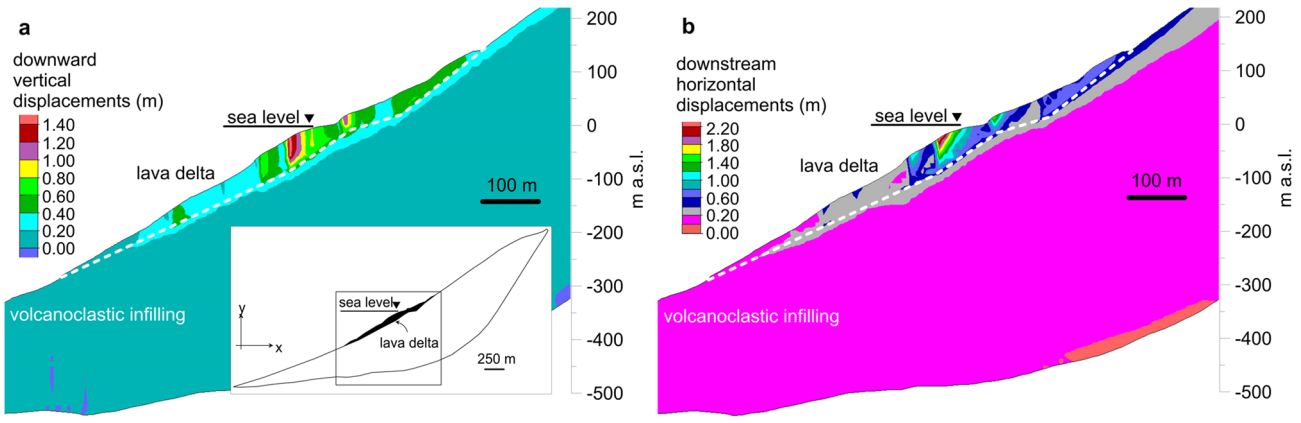

Fig. 7 Displacements produced by the lava delta emplacement: horizontal (**a**) and vertical (**b**) component

Table 2 Geotechnical properties of the lava delta utilized in the numerical model

ρ_d (Mg/m^3)	E (GPa)	v (–)	σ_{ci} (kPa)	m_i (–)	GSI (–)	c_b (kPa)	φ_b (°)
2.12	1.47	0.25	34	15.4	35	120	40.8

and steeper part of the lava delta emplaced within the 2002 landslide scar. These slope failures are likely triggered by severe storm-waves that struck the NW flank of Stromboli during winter months, leading to the progressive dismantling of lava delta, similarly to what happened for similar volcanic structures during the recent evolution of the SdF (Marsella et al. 2012). Moreover, the computed displacements are quite comparable with the values of subsidence measured for the subaerial part of the lava delta in the central sector of the SdF (facing the 2002 submarine landslide scar) through Space-borne SAR data over the period 2010–2016 (Di Traglia et al. 2018b).

Final remarks

The present study evidences how frequent and dangerous can be small-scale landslides affecting volcanic flanks, because they can directly impact coastal or offshore infrastructures (cable break) or create local but devastating tsunamis. So far, most of the studies relies on the detection and monitoring of subaerial slope failures, but repeated multibeam surveys and acoustic monitoring have demonstrated how frequent small-scale landslides can be also in submarine setting. In this respect, the submarine part of the Sciara del Fuoco at Stromboli volcano can be considered as a natural laboratory for their study. The remarkable slope dip and its thick volcaniclastic infilling, unceasingly fed by the products of volcanic activity funnelled into the sea, are predisposing factors for development of slope failures varying in extent and in recurrence time. The morpho-bathymetric monitoring of the Sciara del Fuoco in the period 2002–2013 has evidenced a marked and rapid morphological evolution of this part of the volcano flank, especially during volcanic crisis (effusive eruptions and paroxysms) that interrupt the "normal" Strombolian activity. Over the monitoring period, the submarine part of the SdF has been repeatedly affected by slope failures with different size, such as the tsunamigenic landslide occurred on 30th December 2002 or the smaller slope failures that are progressively dismantling the 2007 lava delta. This study is mainly focused on the instability phenomena involving some millions of cubic meters that mostly occur when undrained conditions establish in the submarine slope (i.e. if sudden strain/stress increments occur) thus promoting static liquefaction. Differently, the likelihood of large failures under drained condition is low, according to slope stability analyses and the shear strength behaviour of the volcaniclastic material.

Based on the experience gained during the 2002 and 2007 eruptions, this study supports the following evidence:

- Magma thrust associated with dyke intrusions in the upper part of the slope, comparable with that observed at the onset of the 2002 and 2007 flank eruptions, is not able to generate shear stress increments in the submarine slope sufficient to generate large failures (1a in Fig. 5), but it can trigger a complex chain of eruption-driven instability processes that can eventually destabilize the submarine slope, as observed during the 2002 event (1b in Fig. 5). This does not exclude that intrusions with overpressures higher that those observed in the monitored eruptions can lead to the destabilization of the entire flank of the volcano;
- The load applied to the submarine volcaniclastic deposit by the emplacement of a lava delta (as the one formed in 2007) mainly induces displacements at a relatively low rate localized within the delta itself and a couple of tens of meters of the underlying volcaniclastic deposit (2a in Fig. 5). This setting leads to progressive settlements of the delta and its dismantling through small- and medium-scale slope failures. However, if higher effusion rates maintain for a long period or larger deltas are built, their effect could unavoidably be different (2b in Fig. 5).

Further sedimentological and geotechnical data and analyses are required to better understand the stability of the submarine portion of the SdF, especially in relation to the occurrence, distribution and geotechnical characteristics of the sandy volcaniclastic levels within the submarine slope deposit. These horizons could act as weak layers for initiation of instability processes. However, this study provides a first assessment of the main triggering mechanisms for small-scale submarine slope failures at Stromboli, a very important issue in consideration of the very active volcanic setting and the widespread exploitation of its coastlines for touristic purposes during the summer season. More generally, this review can be useful for all the researchers and planners working on small-scale landslides in volcanic settings.

Acknowledgements Marine surveys around Stromboli have been carried out in the framework of researches financed by the Italian INGV (National Institute of Geophysics and Volcanology) and DPC (Civil Protection Department). Crews of R/V Urania, Universitatis and Thetis are gratefully acknowledged along with those people taking part in the surveys. Two anonymous reviewers and Federico Di Traglia are gratefully acknowledged for their comments that helped improving the quality of the paper.

References

Acocella V (2005) Modes of sector collapse of volcanic cones: Insights from analogue experiments. J Geophys Res Solid Earth 110(B2)

Acocella V, Neri M, Scarlato P (2006) Understanding shallow magma emplacement at volcanoes: orthogonal feeder dikes during the 2002–2003 Stromboli (Italy) eruption. Geophys Res Lett 33(17)

Allstadt KE, Matoza RS, Lockhart AB, Moran SC, Caplan-Auerbach J, Haney MM, Thelen WA, Malone SD (2018) Seismic and

acoustic signatures of surficial mass movements at volcanoes. J Volcanol Geoth Res 364:76–106
Andronico D, Taddeucci J, Cristaldi A, Miraglia M, Scarlato P, Gaeta M (2013) The 15 March 2007 paroxysm of Stromboli: video-image analysis, and textural and compositional features of the erupted deposit. Bull Volcanol 75:1–19
Apuani T, Corazzato C (2009) Numerical model of the Stromboli volcano (Italy) including the effect of magma pressure in the dyke system. Rock Mech Rock Eng 42(1):53–72
Apuani T, Corazzato C, Cancelli A, Tibaldi A (2005a) Physical and mechanical properties of rock masses at Stromboli: a dataset for volcano instability evaluation. Bull Eng Geol Env 64(4):419
Apuani T, Corazzato C, Cancelli A, Tibaldi A (2005b) Stability of a collapsing volcano (Stromboli, Italy): limit equilibrium analysis and numerical modelling. J Volcanol Geoth Res 144(1–4):191–210
Babonneau N, Delacourt C, Cancouët R, Sisavath E, Bachèlery P, Mazuel A, Jorry SJ, Deschamps A, Ammann J, Villeneuve N (2013) Direct sediment transfer from land to deep-sea: insights into shallow multibeam bathymetry at La Réunion Island. Mar Geol 346:47–57
Baldi P, Bosman A, Chiocci FL, Marsella M, Romagnoli C, Sonnessa A (2008) Integrated subaerial-submarine morphological evolution of the Sciara del Fuoco after the 2002 landslide. In: The Stromboli Volcano: An Integrated Study of the 2002–2003 Eruption. American Geophysical Union, Geophysical Monograph Series, 171–182
Barberi F (1993) Volcanic hazard assessment at Stromboli based on review of historical data. Acta Vulcanol 3:173–187
Beget JE, Kienle J (1992) Cyclic formation of debris avalanche at Mt St Augustine volcano. Nature 356:701–704
Bertagnini A, Métrich N, Landi P, Rosi M (2003) Stromboli volcano (Aeolian Archipelago, Italy): an open window on the deep-feeding system of a steady state basaltic volcano. J Geophys Res Solid Earth 108(B7)
Bertagnini A, Di Roberto A, Pompilio M (2011) Paroxysmal activity at Stromboli: lessons from the past. Bull Volcanol 73(9):1229–1243
Boldini D, Wang F, Sassa K, Tommasi P (2009) Application of large-scale ring shear tests to the analysis of tsunamigenic landslides at the Stromboli volcano, Italy. Landslides 63:231–240
Bonaccorso A, Calvari S, Garfì G, Lodato L, Patanè D (2003) Dynamics of the December 2002 flank failure and tsunami at Stromboli volcano inferred by volcanological and geophysical observations. Geophys Res Lett 30(18)
Bosman A, Chiocci FL, Romagnoli C (2009) Morpho-structural setting of Stromboli volcano, revealed by high-resolution bathymetry and backscatter data of its submarine portions. Bull Volcanol. https://doi.org/10.1007/s00445-009-0279-5
Bosman A, Casalbore D, Romagnoli C, Chiocci FL (2014) Formation of an 'a'ā lava delta: insights from time-lapse multibeam bathymetry and direct observations during the Stromboli 2007 eruption. Bull Volcanol 76(7):838
Bosman A, Casalbore D, Anzidei M, Muccini F, Carmisciano C, Chiocci FL (2015) The first ultra-high resolution digital Terrain model of the shallow-water sector around Lipari Island (Aeolian Islands, Italy). Ann Geophys 58:2. https://doi.org/10.4401/ag-6746
Boudon G, Le Friant A, Komorowski JC, Deplus C, Semet M (2007) Volcano flank instability in the Lesser Antilles Arc: diversity of scale, processes, and temporal recurrence. J Geophys Res 112:B08205. https://doi.org/10.1029/2006JB004674
Brantley SR, Scott WE, Vancouver W (1993) The danger of collapsing lava domes: lessons for Mount Hood Oregon. US Geol Surv Earthq Volcanol 24:244–269
Calvari S, Spampinato L, Lodato et al (2005) Chronology and complex volcanic processes during the 2002–2003 flank eruption at Stromboli volcano (Italy) reconstructed from direct observations and surveys with a handheld thermal camera. J Geophys Res Solid Earth 110(B2)
Calvari S, Spampinato L, Lodato L (2006) The 5 April 2003 vulcanian paroxysmal explosion at Stromboli volcano (Italy) from field observations and thermal data. J Volcanol Geoth Res 149(1–2):160–175
Calvari S, Lodato L, Steffke A, Cristaldi A, Harris AJ, Spampinato L, Boschi E (2010) The 2007 Stromboli eruption: event chronology and effusion rates using thermal infrared data. J Geophys Res Solid Earth 115(B4)
Caplan-Auerbach J, Fox CG, Duennebier FK (2001) Hydroacoustic detection of submarine landslides on Kilauea volcano. Geophys Res Lett 28(9):1811–1813
Caplan-Auerbach J, Dziak RP, Bohnenstiehl DR, Chadwick WW, Lau TK (2014) Hydroacoustic investigation of submarine landslides at West Mata volcano Lau Basin. Geophys Res Lett 41(16):5927–5934
Carter L, Gavey R, Talling PJ, Liu JT (2014) Insights into submarine geohazards from breaks in subsea telecommunication cables. Oceanography 27:58–67
Casagli N, Tibaldi A, Merri A, Del Ventisette C, Apuani T, Guerri L, Tarchi D (2009) Deformation of Stromboli Volcano (Italy) during the 2007 eruption revealed by radar interferometry, numerical modelling and structural geological field data. J Volcanol Geoth Res 182(3–4):182–200
Casalbore D, Romagnoli C, Chiocci FL, Frezza V (2010) Morpho-sedimentary characters of volcaniclastic apron around Stromboli volcano (Italy). Mar Geol 3–4:132–148
Casalbore D, Romagnoli C, Bosman A, Chiocci FL (2011) Potential tsunamigenic landslides at Stromboli Volcano (Italy): insight from marine DEM analysis. Geomorphology 126:42–50
Casalbore D, Bosman A, Chiocci FL (2012) Study of recent small-scale landslides in geologically active marine areas through repeated multibeam surveys: examples from the southern Italy. Submarine mass movements and their consequences. Springer, Dordrecht, pp 573–582
Casalbore D, Romagnoli C, Pimentel A, Quartau R, Casas D, Ercilla G, Hipolito A, Sposato A, Chiocci FL (2015) Volcanic, tectonic and mass-wasting processes offshoreTerceira island (Azores) revealed by high-resolution seafloor mapping. Bull Volcanol 77(3)
Casalbore D, Bosman A, Romagnoli C, Di Filippo M, Chiocci FL (2016a) Morphology of Lipari offshore (Southern Tyrrhenian Sea). Journal of Maps 12(1):77–86
Casalbore D, Bosman A, Martorelli E, Sposato FL, Chiocci FL (2016b) Mass wasting features on the submarine flanks of Ventotene volcanic edifice (Tyrrhenian Sea, Italy). In: Krastel et al. (eds) Submarine mass movements and their consequences, 37, pp 285–293
Casalbore D, Falese F, Martorelli E, Romagnoli C, Chiocci FL (2017) Submarine depositional terraces in the Tyrrhenian sea as a proxy for paleo-sea level reconstruction: problems and perspective. Quat Int 439:169–180
Casalbore D, Romagnoli C, Bosman A, Anzidei M, Chiocci FL (2018) Coastal hazard due to submarine canyons in active insular volcanoes: examples from Lipari Island (southern Tyrrhenian Sea). J Coast Conserv 22(5):989–999
Chadwick Jr WW, Wright IC, Schwarz-Schampera U, Hyvernaud O, Reymond D, De Ronde CEJ (2008) Cyclic eruptions and sector collapses at Monowai submarine volcano, Kermadec arc: 1998–2007. Geochem Geophys Geosyst 9(10)
Chadwick WW Jr, Dziak RP, Haxel JH, Embley RW, Matsumoto H (2012) Submarine landslide triggered by volcanic eruption recorded by in situ hydrophone. Geology 40(1):51–54

Chigira M (2002) Geologic factors contributing to landslide generation in a pyroclastic area: August 1998 Nishigo Village Japan. Geomorphology 46(1–2):117–128

Chiocci FL, Romagnoli C, Tommasi P, Bosman A (2008) The Stromboli 2002 tsunamigenic submarine slide: characteristics and possible failure mechanisms. J Geophys Res 113:B10102. https://doi.org/10.1029/2007JB005172

Chiocci FL, Romagnoli C, Bosman A (2008) Morphologic resilience and depositional processes due to the rapid evolution of the submerged Sciara del Fuoco (Stromboli island) after the December 2002 submarine slide and tsunami. Geomorphology 100(3/4):356–365

Clare MA, Le Bas T, Price DM, Hunt JE, Sear D, Cartigny MJB, Vellinga A, Symons W, Firth C, Cronin S (2018) Complex and cascading triggering of submarine landslides and turbidity currents at volcanic islands revealed from integration of high-resolution onshore and offshore surveys. Front Earth Sci. https://doi.org/10.3389/feart.2018.00223

Coombs ML, White SM, Scholl DW (2007) Massive edifice failure at Aleutian Arc volcanoes. Earth Planet Sci Lett 3–4:403–418

Costa ACG, Marques FO, Hildenbrand A, Sibrant ALR, Catita CMS (2014) Large-scale catastrophic flank collapses in a steep volcanic ridge: the Pico–Faial Ridge, Azores Triple Junction. J Volcanol Geoth Res 272:111–125

Costa ACG, Hildenbrand A, Marques FO, Sibrant ALR, de Campos AS (2015) Catastrophic flank collapses and slumping in Pico Island during the last 130 kyr (Pico-Faial ridge, Azores Triple Junction). J Volcanol Geoth Res 302:33–46

Crosta GB, Imposimato S, Roddeman D, Chiesa S, Moia F (2005) Small fast-moving flow-like landslides in volcanic deposits: the 2001 Las Colinas Landslide (El Salvador). Eng Geol 79(3–4):185–214

de Vita S, Sansivero F, Orsi G, Marotta E (2006) Cyclical slope instability and volcanism related to volcano-tectonism in resurgent calderas: the Ischia island (Italy) case study. Eng Geol 86(2–3):148–165

de Vries BVW, Davies T (2015) Landslides, debris avalanches, and volcanic gravitational deformation. The encyclopedia of volcanoes. Academic Press, Amsterdam, pp 665–685

Deplus C, Le Friant A, Boudon G, Komorowski JC, Villemant B, Harford C, Ségoufin J, Cheminée JL (2001) Submarine evidence for large-scale debris avalanches in the Lesser Antilles Arc. Earth Planet Sci Lett 192:145–157

Devoli G, Cepeda J, Kerle N (2009) The 1998 Casita volcano flank failure revisited—New insights into geological setting and failure mechanisms. Eng Geol 105(1–2):65–83

Di Roberto A, Rosi M, Bertagnini A, Marani MP, Gamberi F (2010) Distal turbidites and tsunamigenic landslides of Stromboli volcano (Aeolian Islands, Italy). Submarine mass movements and their consequences. Springer, Dordrecht, pp 719–731

Di Roberto A, Bertagnini A, Pompilio M, Bisson M (2014) Pyroclastic density currents at Stromboli volcano (Aeolian Islands, Italy): a case study of the 1930 eruption. Bull Volcanol 76(6):827

Di Traglia F, Calvari S, D'Auria L et al (2018) The 2014 Effusive eruption at stromboli: new insights from in situ and remote-sensing measurements. Remote Sens 10(12):2035

Di Traglia F, Nolesini T, Solari L, Ciampalini A, Frodella W, Steri D, Allotta B, Rindi A, Marini L, Monni N (2018) Lava delta deformation as a proxy for submarine slope instability. Earth Planet Sci Lett 488:46–58

Di Traglia F, Bartolini S, Artesi E et al (2018) Susceptibility of intrusion-related landslides at volcanic islands: the Stromboli case study. Landslides 15(1):21–29

Di Traglia F, Nolesini T, Ciampalini A, Solari L, Frodella W, Bellotti F, Fumagalli A, De Rosa G, Casagli N (2018) Tracking morphological changes and slope instability using spaceborne and ground-based SAR data. Geomorphology 300:95–112

Francalanci L, Lucchi F, Keller J, De Astis G, Tranne CA (2013) Eruptive, volcano-tectonic and magmatic history of the Stromboli volcano (north-eastern Aeolian archipelago). Geological Society, London, Memoirs 37(1):397–471

Freundt A (2003) Entrance of hot pyroclastic flows into the sea: experimental observations. Bull Volcanol 65:144–164. https://doi.org/10.1007/s00445-002-0250-1

Galderisi A, Bonadonna C, Delmonaco G et al (2013) Vulnerability assessment and risk mitigation: the case of Vulcano Island, Italy. Landslide science and practice. Springer, Berlin, Heidelberg, pp 55–64

Gillot PY, Keller J (1993) Radiochronological dating of Stromboli. Acta Vulcanol 3:69–77

Guthrie RH, Friele P, Allstadt K, Roberts N, Evans SG, Delaney KB, Roche D, Clague JJ, Jakob M (2012) The 6 August 2010 Mount Meager rock slide-debris flow, Coast Mountains, British Columbia: characteristics, dynamics, and implications for hazard and risk assessment. Nat Hazards Earth Syst Sci 12:1277–1294

Hart K, Carey S, Sigurdsson H, Sparks RSJ, Robertson RE (2004) Discharge of pyroclastic flows into the sea during the 1996–1998 eruptions of the Soufrière Hills volcano Montserrat. Bull Volcanol 66(7):599–614

Hayashi JN, Self S (1992) A comparison of pyroclastic flow and debris avalanche mobility. J Geophys Res Solid Earth 97(B6):9063–9071

Hildenbrand A, Marques FO, Catalão J, Catita CMS, Costa ACG (2012) Large-scale active slump of the southeastern flank of Pico Island. Azores Geol 40(10):939–942

Hildenbrand A, Marques FO, Catalão J (2018) Large-scale mass wasting on small volcanic islands revealed by the study of Flores Island (Azores). Sci Rep 8(1):1–11

Hoek E, Carranza-Torres C, Corkum B (2002) Hoek-Brown failure criterion-2002 edition. Proc NARMS-Tac 1(1):267–273

Hürlimann M, Ledesma A, Martı J (2001) Characterisation of a volcanic residual soil and its implications for large landslide phenomena: application to Tenerife Canary Islands. Eng Geol 59(1–2):115–132

Itasca (2011) FLAC—Fast Lagrangian Analysis of Continua—Version 7.0. User's Guide. Itasca Consulting Group, Minneapolis

Karstens J, Berndt C, Urlaub M et al (2019) From gradual spreading to catastrophic collapse–reconstruction of the 1888 Ritter Island volcanic sector collapse from high-resolution 3D seismic data. Earth Planet Sci Lett 517:1–13

Keating BH, McGuire WJ (2000) Island edifice failures and associated tsunami hazards. Pure Appl Geophys 157:899–955

Kidd RB, Lucchi RG, Gee M, Woodside JM (1998) Sedimentary processes in the Stromboli Canyon and Marsili Basin, SE Tyrrhenian Sea: results from side-scan sonar surveys. Geo-Mar Lett 18(2):146–154

Kokelaar P, Romagnoli C (1995) Sector collapse, sedimentation and clast-population evolution at an active island-arc volcano: Stromboli. Italy Bull Volcanol 57:240–262

Leat PT, Tate AJ, Tappin DR, Day SJ, Owen MJ (2010) Growth and mass wasting of volcanic centers in the northern South Sandwich arc, South Atlantic, revealed by new multibeam mapping. Mar Geol 275(1–4):110–126

Legros F (2002) The mobility of long-runout landslides. Eng Geol 63:301–331

Madonia P, Cangemi M, Olivares L, Oliveri Y, Speziale S, Tommasi P (2019) Shallow landslide generation at La Fossa cone, Vulcano island (Italy): a multidisciplinary perspective. Landslides 16(5):921–935

Maramai A, Graziani L, Tinti S (2005) Tsunamis in the Aeolian Islands (southern Italy): a review. Mar Geol 215(1/2):11–21

Marani MP, Gamberi F, Rosi M, Bertagnini A, Di Roberto A (2008) Deep-sea deposits of the stromboli 30 december 2002 landslide the stromboli volcano: an integrated study of the 2002–2003 eruption. Geophys Monogr Ser. https://doi.org/10.1029/182GM14

Marani MP, Gamberi F, Rosi M, Bertagnini A, Di Roberto A (2009) Subaqueous density flow processes and deposits of an island volcano landslide (Stromboli Island, Italy). Sedimentology 56(5):1488–1504

Marinos V, Marinos P, Hoek E (2005) The geological strength index: applications and limitations. Bull Eng Geol Environ 64:55–65. https://doi.org/10.1007/s10064-004-0270-5

Marsella M, Proietti C, Sonnessa A, Coltelli M, Tommasi P, Bernardo E (2009) The evolution of the Sciara del Fuoco subaerial slope during the 2007 Stromboli eruption: Relation between deformation processes and effusive activity. J Volcanol Geoth Res 182(3–4):201–213

Marsella M, Baldi P, Coltelli M, Fabris M (2012) The morphological evolution of the Sciara del Fuoco since 1868: reconstructing the effusive activity at Stromboli volcano. Bull Volcanol 74(1):231–248

Marsella M, Salino A, Scifoni S, Sonnessa A, Tommasi P (2013) Stability conditions and evaluation of the runout of a potential landslide at the northern flank of La Fossa active volcano, Italy. Landslide science and practice. Springer, Berlin, Heidelberg, pp 309–314

McGuire WJ (2003) Volcano instability and lateral collapse. Revista 1:33–45

Meireles RP, Quartau R, Ramalho RS, Rebelo AC, Madeira J, Zanon V, Ávila SP (2013) Depositional processes on oceanic island shelves—evidence from storm-generated Neogene deposits from the mid-North Atlantic. Sedimentology 60(7):1769–1785

Mercalli G (1907).I vulcani attivi della terra: morfologia-dinamismo-prodotti-distribuzione geografica-cause. Con 82 incisioni e 26 tavle. U. Hoepli.

Métrich N, Bertagnini A, Landi P, Rosi M, Belhadj O (2005) Triggering mechanism at the origin of paroxysms at Stromboli (Aeolian Archipelago, Italy): the 5 April 2003 eruption. Geophys Res Lett 32(10)

Mitchell NC, Masson DG, Watts AB, Gee MJR, Urgeles R (2002) The morphology of the submarine flanks of volcanic ocean islands. A comparative study of the Canary and Hawaiian hotspot islands. J Volcanol Geoth Res 115:83–107

Mitchell NC, Beier C, Rosin PL, Quartau R, Tempera F (2008). Lava penetrating water: submarine lava flows around the coasts of Pico Island, Azores. Geochem Geophys Geosyst 9(3)

Moore JG, Normark WR, Holcomb RT (1994) Giant Hawaiian landslides. Annu Rev Earth Planet Sci 22:119–144

Oehler JF, Lénat JF, Labazuy P (2008) Growth and collapse of the Reunion Island volcanoes. Bull Volcanol 70:717–742

Olivares L, Tommasi P (2008). The role of suction and its changes on stability of steep slopes in unsaturated granular soils. Special Lecture. In: Chen Z., Zhang J., Ho K Wu F, Li Z (eds) Landslides and engineered slopes. From the past to the future, Proceedings 10th International Symposium on Landslides and Engineered Slopes, Xi'an, China, CRC Press/Balkema, Leiden, 1, 203–215. ISBN 978-0-415-41194-3

Paguican EMR, de Vries BVW, Lagmay AMF (2012) Volcano-tectonic controls and emplacement kinematics of the Iriga debris avalanches (Philippines). Bull Volcanol 74(9):2067–2081

Paris R, Switzer AD, Belousova M, Belousov A, Ontowirjo B, Whelley PL, Ulvrova M (2014) Volcanic tsunami: a review of source mechanisms, past events and hazards in Southeast Asia (Indonesia, Philippines, Papua New Guinea). Nat Hazards 70:447–470

Pistolesi, M, Rosi, M, Pioli, L, Renzulli, A, Bertagnini, A, Andronico, D (2008) The paroxysmal event and its deposits. The Stromboli Volcano An integrated study of the 2002–2003 eruption, 317–330

Pistolesi, M, Delle Donne, D, Pioli, L, Rosi, M, & Ripepe, M (2011) The 15 March 2007 explosive crisis at Stromboli volcano, Italy: assessing physical parameters through a multidisciplinary approach. J Geophys Res Solid Earth 116(B12)

Del Potro R, Hürlimann M (2008) Geotechnical classification and characterisation of materials for stability analyses of large volcanic slopes. Eng Geol 98(1–2):1–17

Quartau R, Trenhaile AS, Mitchell NC, Tempera F (2010) Development of volcanic insular shelves: Insights from observations and modelling of Faial Island in the Azores Archipelago. Mar Geol 275:66–83

Quartau R, Tempera F, Mitchell NC, Pinheiro LM, Duarte H, Brito PO, Bates R, Monteiro JH (2012) Morphology of the Faial Island shelf (Azores): the interplay between volcanic, erosional, depositional, tectonic and mass-wasting processes. Geochem Geophys Geosy 13:Q04012

Quartau R, Hipolito A, Romagnoli C, Casalbore D, Madeira J, Tempera F, Roque C, Chiocci FL (2014) The morphology of insular shelves as a key for understanding the geological evolution of volcanic islands: insights from Terceira Island (Azores). Geochem Geophys Geosyst 15:1801–1826

Quartau R, Ramalho RS, Madeira J, Santos R, Rodrigues A, Roque C, Carrara G, da Silveir AB (2018) Gravitational, erosional and depositional processes on volcanic ocean islands: Insights from the submarine morphology of Madeira Archipelago. Earth Planet Sci Lett 482:288–299

Romagnoli C, Mancini F, Brunelli R (2006) Historical Shoreline Changes at an Active Island Volcano: Stromboli, Italy. J Coast Res 224:739–749

Romagnoli C, Kokelaar P, Casalbore D, Chiocci FL (2009a) Lateral collapses and active sedimentary processes on the northwestern flank of Stromboli volcano Italy. Mar Geol 265:101–119

Romagnoli C, Casalbore D, Chiocci FL, Bosman A (2009b) Offshore evidence of largescale lateral collapses on the eastern flank of Stromboli, Italy, due to structurallycontrolled, bilateral flank instability. Mar Geol 262(1–4):1–13

Romagnoli C, Casalbore D, Chiocci FL (2012) La Fossa Caldera breaching and submarine erosion (Vulcano island, Italy). Mar Geol 303:87–98

Romagnoli C, Casalbore D, Bortoluzzi G, Bosman A, Chiocci FL, D'Oriano F, Gamberi F, Ligi M, Marani M (2013) Bathymorphological setting of the Aeolian islands. In: Lucchi F, Peccerillo A, Keller J, Tranne CA, Rossi PL (eds) The Aeolian Islands Volcanoes, vol 37. Geological Society London Memoirs, London, pp 27–36

Rosi M, Bertagnini A, Harris AJL, Pioli L, Pistolesi M, Ripepe M (2006) A case history of paroxysmal explosion at Stromboli: timing and dynamics of the April 5, 2003 event. Earth Planet Sci Lett 243(3–4):594–606

Rosi M, Levi ST, Pistolesi M, Bertagnini A, Brunelli D, Cannavò V, Di Renzoni A, Ferranti F, Renzulli A, Yoon D (2019) Geoarchaeological evidence of middle-age tsunamis at Stromboli and consequences for the tsunami Hazard in the southern Tyrrhenian Sea. Sci Rep 9(1):677

Rotonda T, Tommasi P, Boldini D (2009) Geomechanical characterization of the volcaniclastic material involved in the 2002 landslides at Stromboli. J Geotech Geoenviron Eng 136(2):389–401

Rotonda T, Tommasi P, Boldini D (2010) Geomechanical characterization of the volcaniclastic material involved in the 2002 landslides at Stromboli. J Geotech Geoenviron Eng 136(2):389–401

Salvatici T, Di Roberto A, Traglia Di et al (2016) From hot rocks to glowing avalanches: numerical modelling of gravity-induced pyroclastic density currents and hazard maps at the Stromboli Volcano (Italy). Geomorphology 273:93–106

Santos R, Quartau R, da Silveira AB, Ramalho R, Rodrigues A (2019) Gravitational, erosional, sedimentary and volcanic processes on the submarine environment of Selvagens Islands (Madeira Archipelago, Portugal). Mar Geol 415:105945

Sassa K, Dang K, Yanagisawa H, He B (2016) A new landslide-induced tsunami simulation model and its application to the 1792 Unzen–Mayuyama landslide-and-tsunami disaster. Landslides 13(6):1405–1419

Satake K (2007) Volcanic origin of the 1741 Oshima–Oshima tsunami in the Japan Sea. Earth Planets Space 59(5):381–390

Satake K, Kato Y (2001) The 1741 Oshima–Oshima eruption: extent and volume of submarine debris avalanche. Geophys Res Letts 28(3):427–430

Schaefer LN, Kendrick JE, Oommen T, Lavallée Y, Chigna G (2015) Geomechanical rock properties of a basaltic volcano. Front Earth Sci 3:29

Self S, Rampino M (1981) The 1883 eruption of Krakatau. Nature 292:699–704

Sibrant A, Marques FO, Hildenbrand A (2014) Construction and destruction of a volcanic island developed inside an oceanic rift: Graciosa Island, Terceira Rift Azores. J Volcanol Geotherm Res 284:32–45

Sparks RSJ, Barclay J, Calder ES, Herd RA, Luckett R, Norton GE, Ritchie LJ, Voight B, Woods AW (2002) Generation of a debris avalanche and violent pyroclastic density current on 26 December (Boxing Day) 1997 at Soufriere Hills Volcano, Montserrat. In: Druitt TH, Kokelaar BP (eds) The eruption of Soufriere Hills Volcano, Montserrat, from 1995 to 1999. Geological Society of London, London, pp 409–434

Talling PJ (2014) On the triggers, resulting flow types and frequencies of subaqueous sediment density flows in different settings. Mar Geol 352:155–182

Tappin DR, Watts P, McMurty GM, Lafoy Y, Matsumoto T (2001) The Sissano, Papua New Guinea tsunami of July, 1998—offshore evidence on the source mechanism. Mar Geol 175:1–24

Tibaldi A (2001) Multiple sector collapses at Stromboli volcano, Italy: how they work. Bull Volcanol 63:112–125

Tibaldi A, Vezzoli L (2004) A new type of volcano flank failure: the resurgent caldera sector collapse, Ischia, Italy. Geophys Res Lett 31(14)

Tibaldi A, Corazzato C, Marani M, Gamberi F (2009) Subaerial-submarine evidence of structures feeding magma to Stromboli Volcano, Italy, and relations with edifice flank failure and creep. Tectonophysics 469(1–4):112–136

Tinti S, Maramai A, Armigliato A, Graziani L, Manucci A, Pagnoni G, Zaniboni F (2005) Observations of physical effects from tsunamis of December 30, 2002 at Stromboli volcano, southern Italy. Bull Vulcanol. https://doi.org/10.1007/s00445-005-0021-x

Tinti S, Pagnoni G, Zaniboni F (2006) The landslides and tsunamis of the 30th of December 2002 in Stromboli analysed through numerical simulations. Bull Volcanol 68(5):462–479

Tommasi P, Boldini D, Rotonda T (2005) Preliminary characterization of the volcaniclastic material involved in the 2002 landslides at Stromboli. In: Proceedings of the International Conference on Problematic Soils GEOPROB 2005, Famagusta, Bilsel and Nalbantoglu (eds), 3:1093–1101

Tommasi P, Baldi P, Chiocci FL, Coltelli M, Marsella M, Romagnoli C (2008) Slope failure induced by the December 2002 eruption at Stromboli volcano. In: Calvari S, Inguaggiato S, Puglisi G, Ripepe M, Rosi M (eds) The Stromboli Volcano: an integrated study of the 2002–2003 eruption Geophysical Monograph Series. AGU, Washington, pp 129–145

Tommasi P, Rotonda T, Verrucci L, Graziani A, Boldini D (2018) Geotechnical analysis of instability phenomena at active volcanoes: two case histories in Italy. Landslides and Engineered Slopes. Experience theory and practice. CRC Press, Boca Raton, pp 53–78

Trofimovs J, Amy L, Boudon G, Deplus C, Doyle E, Fournier N, Hart MB, Komorowski J-C, Le Friant A, Lock EJ, Pudsey C, Ryan G, Sparks RSJ, Talling PJ (2006) Submarine pyroclastic deposits formed at the Soufrière Hills Volcano, Montserrat (1995–2003): what happens when pyroclastic flows enter the ocean? Geology 34(7):549–552

Trofimovs J, Foster C, Sparks RSJ et al (2012) Submarine pyroclastic deposits formed during the 20th May 2006 dome collapse of the Soufriere Hills Volcano Montserrat. Bull Volcanol 74(2):391–405

Urgeles R, Canals M, Baraza J, Alonso B, Masson D (1997) The most recent megalandslides of the Canary Islands: El Golfo debris avalanche and Canary debris flow, west El Hierro Island. J Geophys Res 102(B9):20305–20323

Valadao P, Gaspar JL, Queiroz G, Ferreira T (2002) Landslides density map of S. Miguel Island, Azores archipelago

Verrucci L, Tommasi P, Boldini D, Graziani A, Rotonda T (2019) Modelling the instability phenomena on the NW flank of Stromboli Volcano (Italy) due to lateral dyke intrusion. J Volcanol Geoth Res 371:245–262

Voight B, Elsworth D (1997) Failure of volcano slopes. Geotechnique 47(1):1–31

Voight B, Le Friant A, Boudon G, Deplus C, Komorowski JC, Lebas E, Trofimovs J (2012) Undrained sediment loading key to long-runout submarine mass movements: Evidence from the Caribbean Volcanic Arc. Submarine mass movements and their consequences. Springer, Dordrecht, pp 417–428

Walter TR, Haghighi MH, Schneider FM et al (2019) Complex hazard cascade culminating in the Anak Krakatau sector collapse. Nature communications 10(1):1–11

Williams R, Rowley P, Garthwaite MC (2019) Reconstructing the Anak Krakatau flank collapse that caused the December 2018 Indonesian tsunami. Geology 47(10):973–976